NONLINEAR ANALYSIS OF A PRESTRESSED STEEL PIPELINE CROSSING

Simone Pontes de Sá Barreto
Depto. de Engenharia Civil, UFPE – Campus, Recife, PE 50740-540, Brazil
sbarreto@ufpe.br

Bernardo Horowitz
Depto. de Engenharia Civil, UFPE – Campus, Recife, PE 50740-540, Brazil
horowitz@ufpe.br

Abstract. An effective solution for elevated pipeline crossings up to 60m is externally prestressed steel tube. For the case study described herein it represents an economy of 12% with respect to the other alternatives. Finite element models of localized stress concentrations at intermediate stiffeners and stiffening ring supports are presented. A shell model with stiffeners is studied to avoid the damaging ovalization due to the prestressing force. In order to asses stresses, a rational simplified method is developed. For the load levels considered the stresses are well below the yield limit of the structural steel used in the pipe. As second order effects are of primary concern nonlinear analyses are studied. Two sources of second order effects are identified: axial force due to prestressing and water internal pressure. A simplified rational method is presented to take into account both effects using critical loads as parameters.

Keywords. *pipeline, tube, prestress, pressure, nonlinear*

1. Introduction

Pipelines frequently have to cross obstacles like rivers, valleys and roads. There are two types of solutions for these crossings: elevated or underground. The choice is mostly dependent on economical reasons. However, in environmental sensitive sites some governmental agencies require crossings to be elevated. The city of Houston for example, prefers elevated crossing as stated in its design manual (Department of Public Works and Engineering, 1999).

In the case of elevated crossings there are two alternative structural solutions: pipelines supported by auxiliary structures or self-supporting pipelines. In this paper, a real case of a self-supporting externally prestressed steel pipeline crossing is studied. Three aspects deserve special consideration: localized stress in the pipe shell due to intermediate stiffeners and stiffening ring supports, ovalization caused by the eccentricity of the anchorage of the prestressing force and geometric nonlinearity due to the application of large prestressing forces and the long span of the crossing.

2. Description of a Prestressed Steel Pipe Crossing

The real case studied is a water pipeline crossing with a total length of 109.50m, composed of three simply supported spans. The central one has 38.60m and the other two 31.47m and 39.42m. The span lengths were dictated by the spans of an adjacent bridge. The internal diameter of the pipeline is 1.225m. The final solution consists of a steel tube, 16mm thick, supported at both ends by stiffened ring supports, Fig. (1). At the middle third sections intermediate stiffeners are provided to act as deviators for two external prestressing cables each consisting of five grease-coated, seven-wire strand encased in a plastic tube, 5/8” in diameter, Fig. (2). The five strands in their turn are encased in a 75mm diameter High Density Polyethylene sheath. The prestressing force in each cable is 70tf.

The prestressing operation starts out by applying 10% of the final force in each cable. Afterwards cement grout is injected under pressure in the High Density Polyethylene sheaths. After the grout is cured the rest of the prestressing force is applied through monostrand jacks at one end of the pipe for the two cables simultaneously. The cables are finally anchored at both ends through special anchorage devices, Fig. (3).

Figure 1. Pipeline

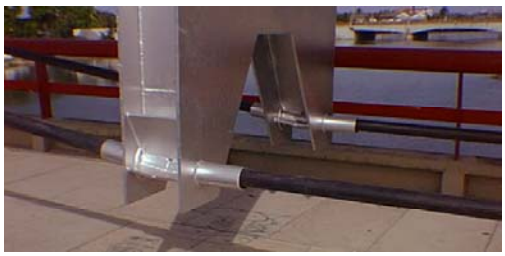

Figure 2. Toroidal deviators

The initial prestressing is required in order for the strands to become straight, and lose their camber. The grout injection servers a double purpose: corrosion protection and maintaining individual strands in their positions over the deviators.

The prestressing cables exert upward forces on the deviators and therefore induce in the pipe shell stresses that oppose those due to the fluid. They also stiffen the tube. We can then expect lower displacements as well as large reduction in flexural stresses as comparable to the tube alone acting as a beam. This solution permits easily free spans up to 60m. In the present case studies show that the prestressed solution is 12% cheaper than the auxiliary supported solution.

The sections below present finite element analysis of the stresses in the pipe shell at the deviator stiffeners due to internal pressure. It also studies stresses in the stiffening ring at the supports, the ovalization of the tube and the nonlinear effects due to the prestressing forces.

3. Localized Stresses at Intermediate Stiffeners

In order to transfer the forces applied by the cables at deviators, intermediate stiffeners are welded to the steel tube. As the pipe is subjected to internal pressure the restraint of radial displacement by the stiffener plates generate localized bending stress in the steel pipe known as rim stresses.

Figure 3. Stiffened ring support and anchorage of the cables

The study below addresses the analysis of these stresses with the following purposes:

- Develop effective finite element models;
- Assess the value of the localized stresses for design purposes and comparison with literature results;
- To assess the influence of flanges welded to stiffening rings.

In order to develop effective finite element meshes two models are studied below: a solid axisymmetric model and a shell model. The first is used as a benchmark for the second. In both cases the mean radius of the shell is 0.6205m, the external radius of the stiffener is 0.974m, its thickness is 16mm, and the internal pressure is 47.4tf/m^2.

3.1. Solid axisymmetric model

In Fig. (4) it is shown the deformed shape of the model and the contours of the longitudinal stresses for the pipe shell only. It can be seen that the maximum normal stress is 1372.52tf/m^2 (13.73MPa).

3.2. Shell model

The most cost effective model for the crossing is composed of shell elements for the pipe shell as well as for stiffeners and flanges. A number of shell models were analyzed. Figure (5) shows one-half of the final proposed model and is composed of isoparametric four-node quadrilateral elements (MSC, 2001).

It has been observed in the solid model that the stiffener's influence regions extend 0.50m symmetrically from its center line. Therefore, a finer mesh was used in this region. According to Cook (1995), at least two elements should be used in the boundary layer given by:

$$b = \sqrt{R \cdot t} \tag{1}$$

where R is the mean radius of the pipe; t is the thickness of the pipe shell. In the present case b = 0.10m and three elements were used.

The deformed shape and the resulting longitudinal stresses are shown in Fig. (5). It can be seen that the maximum normal stress is 1410.05tf/m^2 (14.1 MPa), which is close to the solid model. The difference is less than 3%.

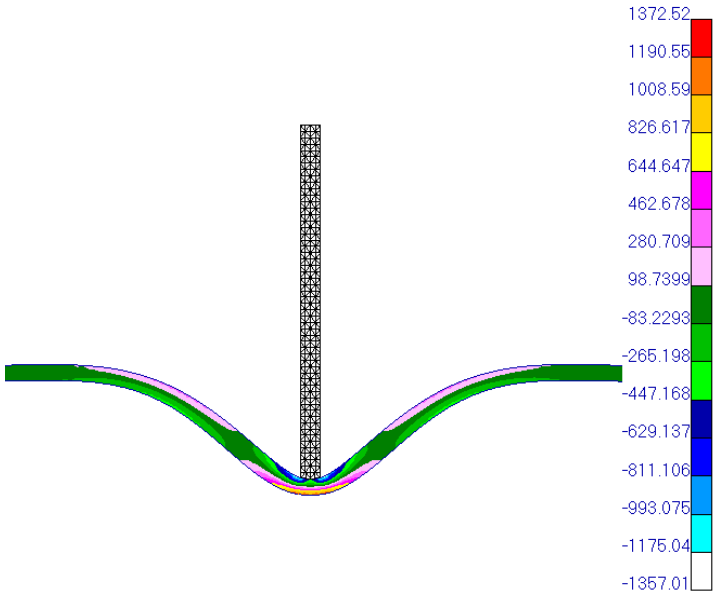

Figure 4. Deformed shape and longitudinal stresses

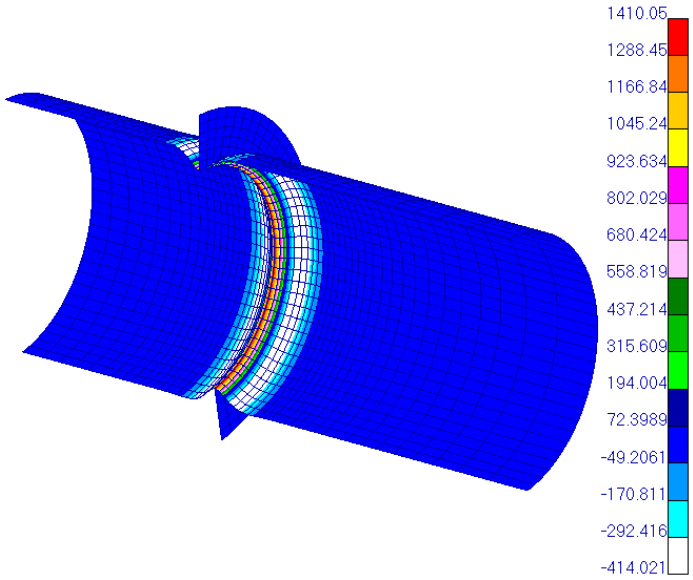

Figure 5. Longitudinal stress and deformed shape

3.3. Comparison

The usual reference for rim stress in waterworks design is an old elasticity theory studied by Pasternak (1926). The maximum rim bending stress in the pipe shell is given by:

$$\sigma_{max} = \frac{1.82 \cdot (Ar - c \cdot t)}{(Ar + 1.56 \cdot t \cdot \sqrt{r \cdot t})} \cdot \frac{p \cdot r}{t} \quad (2)$$

where Ar = area of supporting ring in a plane along the axis of pipe; c = width of circular girder ring; t = thickness of the pipe shell; p = uniform inside pressure; r = mean radius of pipe.

Applying to the present case one gets σ_{max} = 2218tf/m^2 (22.18MPa) which is significantly higher than both finite element results.

3.4. Influence of flanges

In the real case studied here, flanges are welded to the stiffeners. It has not been found direct formulation to account for the presence of flanges. In Fig. (6) it is shown one half of the finite element model analyzed, the deformed shape and stresses. It can be seen that the maximum stress increase to 1514.25tf/m^2 (15.14MPa), a 7.5% increase. Observe also the deformed shape of the flange. The stress at the tip of the flanges is lower that at its center. Therefore, it is not appropriate to simplify the model by lumping the flange area at the outer edge of the stiffener.

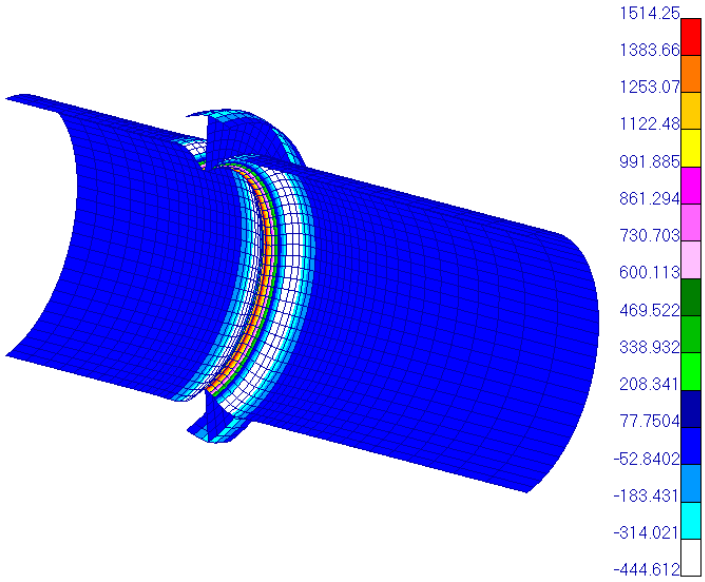

Figure 6. Model with flanges - Deformed shape and longitudinal stress

4. Localized Stresses in Supports

Each span of the pipeline is supported at both ends by stiffened ring supports. A model of one of these stiffened ring supports was analyzed. A quarter of the tube was discretized as shown in Fig. (7a). In one end of the pipe, a vertical uniform load of 50.0707tf/m was applied to the stiffener. In the opposite end, the support is modeled by restraining vertical displacements. The support is allowed to move in the longitudinal direction in order to model the neoprene pad.

In Fig. (7b) it is shown the stresses in the support. The stress at horizontal diameter is 1197.31tf/m^2 (11.97MPa). According to Troitsky (1982), the maximum bending stress (f_1) and the maximum ring stress due to shear forces (f_2) are given by:

$$f_1 = \frac{M \cdot y}{I} \quad (3)$$

$$f_2 = \frac{Q}{4 \cdot Ar} \quad (4)$$

where y = distance from neutral axis to extreme fiber; I = moment of inertia of the supporting ring with respect to the neutral axis; Q = total vertical reaction; Ar = area of supporting ring in a plane along the axis of pipe. M is the maximum possible ring moment and is given by:

$$M = 0.01 \cdot Q \cdot R \quad (5)$$

where R = radius of the neutral axis.

The total maximum stress happens at the horizontal diameter of the ring girder and is given by:

$$f_T = f_1 + f_2 \tag{6}$$

At the present case f_T = 1511tf/m^2 (15.11MPa), which compares favorably with the finite element value at the horizontal diameter.

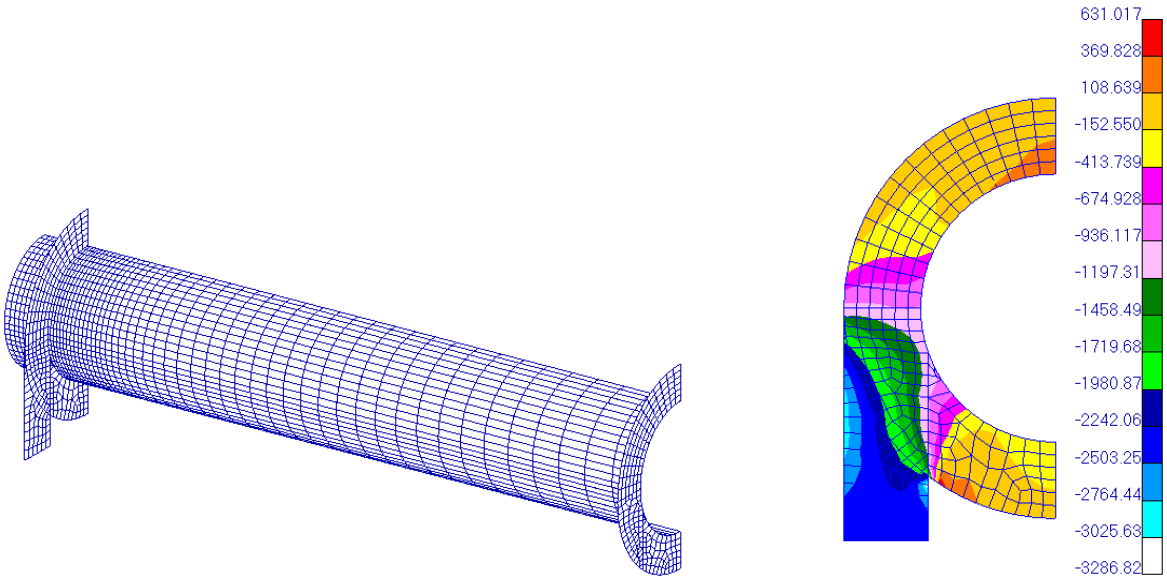

(a) (b)

Figure 7. (a) Finite element mesh; (b) Stress in support

Finite element result does not attain its maximum stress at the horizontal diameter, but at the lower region of the support, and is much higher than the literature result.

In order to study the influence of flanges a finite element model was analyzed. The stresses are shown in Fig. (8). The stress at the horizontal diameter is 1108.67tf/m2 (11.09MPa), which is a decrese of 7.4% in relation to the case without flanges.

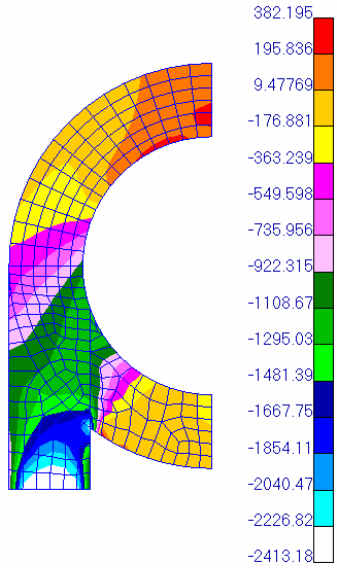

Figure 8. Stress in support with flange

5. Ovalization

Due to the eccentricity of the anchorage of the prestressing force, large moments develop in the pipe shell causing damaging ovalization. Two finite element models are analyzed in order to better understand this problem. It is also

studied the feasibility of special fittings such as stiffeners and stiffening rings. In both cases the mean radius of the shell is 0.6205m, the total length of the tube is 6.205m and its thickness is 16mm.

5.1. Pipe shell without stiffeners

In Fig. (9a) it is shown the finite element model. The thickness to the metal plate H is 50mm and to the other two plates is 25mm. The force applied to the metal plate H is P = 70tf at the distance 0.170m from the pipe shell.

The stresses are shown in Fig. (9b). It can be seen that the maximum stress is 191440.00tf/m^2 (1914.40MPa) which is higher than the steel yield stress (fy = 250MPa). In order to avoid this problem, the section below studies a finite element model of an alternative solution.

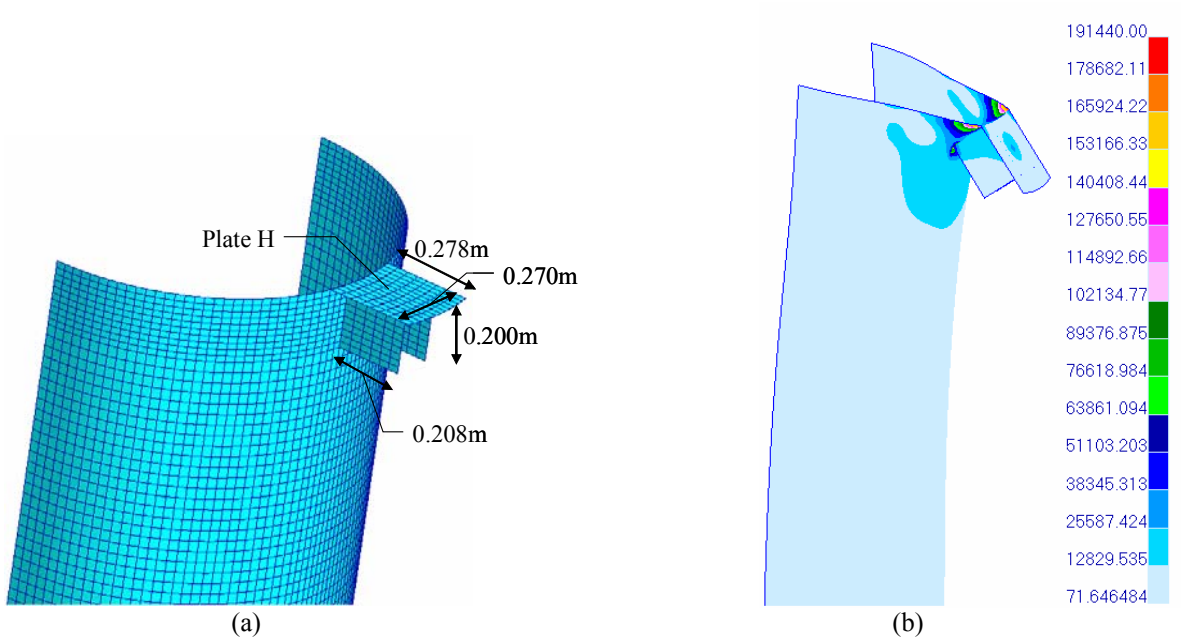

Figure 9. (a) Finite element model; (b) Deformed shape and Von Misses stress

5.2. Pipe shell with stiffeners

A quarter of the model was discretized. In Fig. (10) it is shown the geometry dimensions. A number of stiffeners are located between two stiffening rings and a force of 35tf is applied to a plate, henceforth designated as “plate H” (see Fig. (10)). Table (1) shows the thickness of the metal plates.

In this case the maximum Von Misses stress is 9212.16tf/m^2 (92.12MPa) which is lower than the yield stress (fy = 250MPa) and is 5% of the maximum stress of the model without stiffeners.

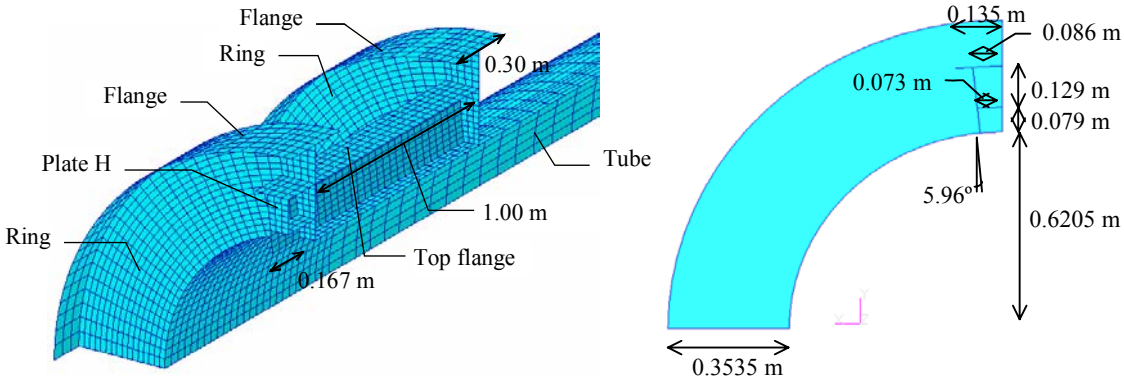

Figure 10. Finite element mesh and model dimension

The membrane forces at the top flange are now studied. The maximum normal force is 117.99tf/m in the case that flanges are used and 118.64tf/m without flanges. Therefore, flanges have no significant influence on results.

Table 1. Thickness of the shells

Shell thickness (mm)	
Tube	16
Flanges	16
Rings	19
Plate H	50
Plates - others	25

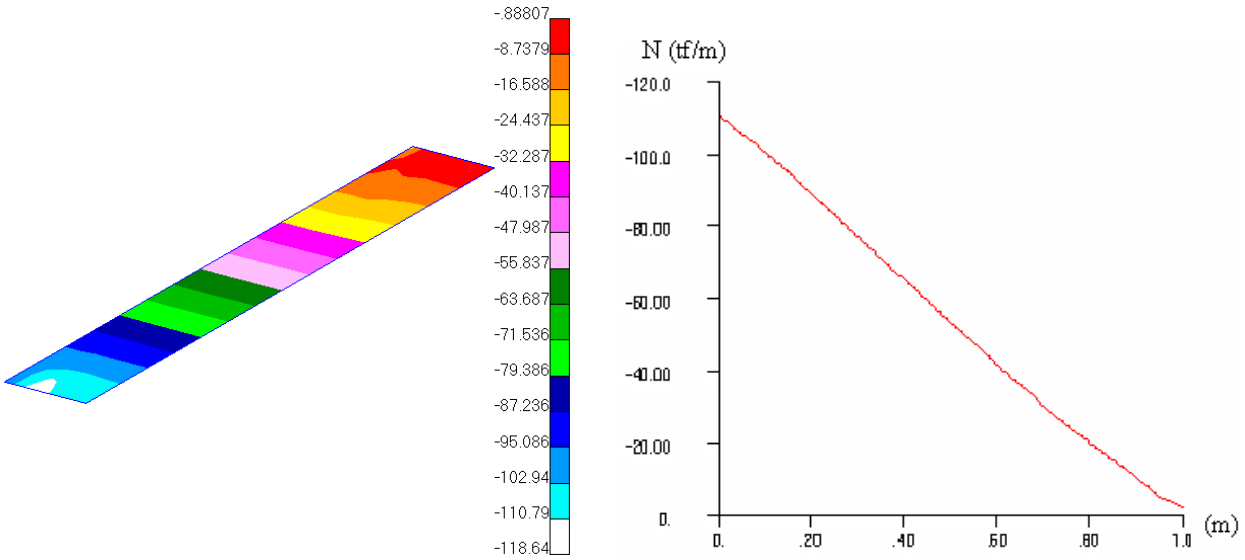

Figure 11. Normal force to the case without flanges

5.2.1. Rational Simplified Method

In this section, a simplified model is proposed to asses the stresses in the top flange for initial design purposes. In this method, the top flange and stiffeners act as a beam simply supported at the stiffening rings, Fig. (12a). Considering the beam section shown in Fig. (12b) the maximum stress at the top flange is given by:

$$\sigma_{\max} = \frac{P}{A} + \frac{M \cdot z}{I} \tag{7}$$

where the normal force P is 70tf, the section area A is 0.0475m^2, the distance z is 0.319m and the moment of inertia I is 2.683E-3m^4. The bending moment M is given by:

$$M = P \cdot e \tag{8}$$

where e is the eccentricity due to the reaction force (R_P) at the end of the tube, where the stresses are assumed uniform, and the applied force P, Fig. (13). In the present case e = 0.371m and M = 25.97tf.m.

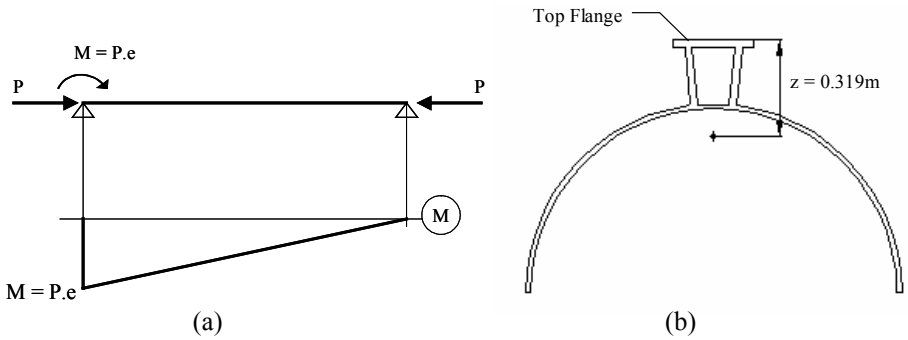

Figure 12. (a) Simplified beam model and diagram of bending moment; (b) Beam section

The maximum membrane normal force in the section is given by:

$$N_{max} = \sigma_{max} \cdot t \tag{9}$$

where the thickness of the top flange t is 25mm. In the present case the result of Eq. (9) is N_{max} = 114.04tf/m which is a good approximation to the result from the finite element analysis (118.64tf/m). The linear variation of the graphic shown in Fig. (11) agrees with the diagram of bending moment of the simplified beam model, Fig. (12a).

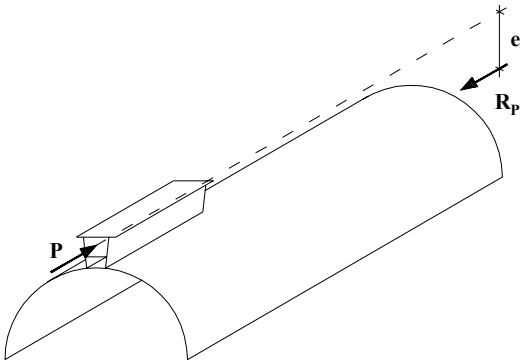

Figure 13. Scheme of forces

6. General behavior

6.1. Full nonlinear model

In this section, a full three-dimensional nonlinear finite element model of the pipeline central span is analyzed. In Fig. (14) it is shown one-half of the pipeline geometry. The thickness of the tube, flanges and deviating stiffeners is 16mm and ring, support ring and set of stiffeners is 19mm. The mean radius of the pipe shell is 0.6205m. The shells are composed of isoparametric four-node quadrilateral elements and the prestressing cables are discretized as beam elements. The neoprene pads in the bottom of the supports are modeled as springs. The vertical constant is k_v = 745tf/m and the horizontal is k_h = 13tf/m.

The pipe is subjected to four loads: self-weight, prestressing, water pressure and wind. The density of the pipe shell is γ_S = 9.45tf/m^3. The prestressing is considered as a temperature drop of –513ºC that is equivalent to the 70tf prestressing force in each cable. The water pressure is modeled as a field that varies with the high between the pipe shell and the maximum level of water in the reservoir, which is 46.9m in relation to the pipe axis. Therefore, it can be said that the pipeline works as a forced conduct. Caution should be exercised in nonlinear analysis to model the water pressure. It is essential that pressures be applied as "follower" forces. Otherwise, a significant error is introduced rendering nonlinear displacement smaller than those of the linear analysis. The wind load is computed according to the code NB-599 (1987). It is applied in the global X direction, as a 0.022tf/m distributed load at the top and bottom generators. Tab. (2) shows the vertical displacement and the components of stress Y and Z with respect to the global coordinate system.

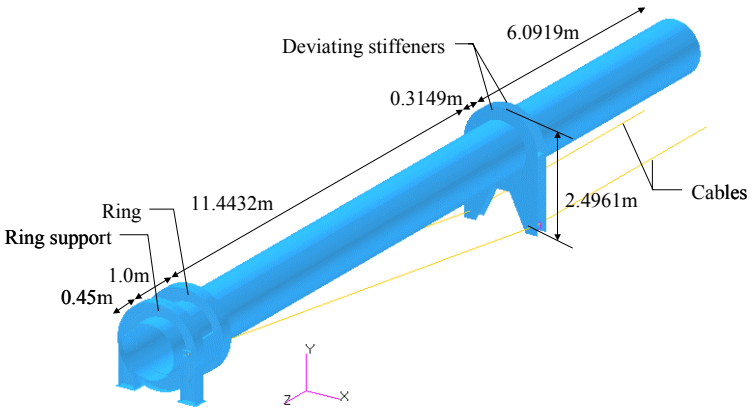

Figure 14. One-half of the pipeline geometry

According to AWA (1987), the maximum stress $\sigma_{max} < f_y/2$, where f_y is the steel yield stress, and the ratio v/L should be lower than 1/360, where v is the vertical displacement and L is the total length of the tube. In the present case, v/L is 1/689 and the maximum stress is lower than half of the yield stress as shown in Fig. (15). Therefore, the proposed design is considered satisfactory.

Table 2. Vertical displacement and stresses from nonlinear analysis

Load Case	Stress (MPa)		Displacement (m)
	σ_Y	σ_Z	
Self-weight + prestressing	56.86	82.76	0.05855
Self-weight + prestressing + water + wind	68.35	87.09	-0.05603

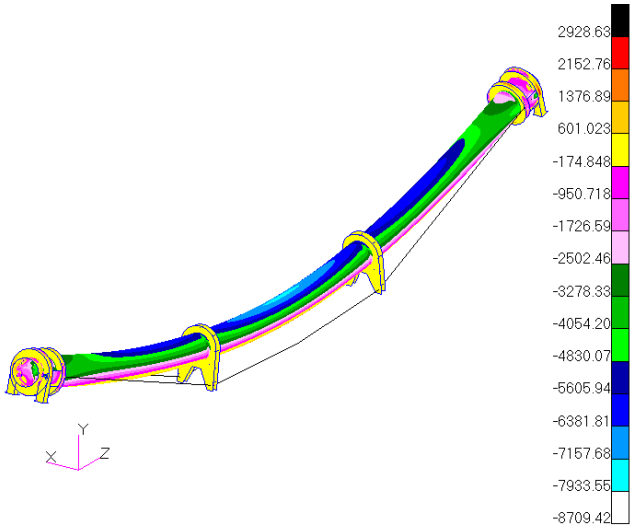

Figure 15. Deformed shape and stress contours (tf/m^2)

6.2. Second order effects

In this section, two cases with different water loads are studied: 1- Water as pressure and 2- Water as distributed vertical load. In both cases self-weight and prestressing are also present. In Tab. (3) it can be seen the linear and nonlinear results for each case studied here.

Table 3. Displacements per load case

Case	Vertical displacement (m)		Nonlinear/Linear
	Linear analysis	Nonlinear analysis	
1	-0.054099	-0.055959	1.034
2	-0.053385	-0.053908	1.0098

As the external loads are of the follower type, extra nonlinearities are induced. There are two effects of second order: due to the axial cable force and due to the effect of the water pressure in the curvature of the tube. This second effect is clear from the nonlinear results for case 1, with a larger amplification of displacements. This is an important effect and should not be neglected in the analysis.

6.2.1. Amplification coefficient

Due to the application of large prestressing forces and the long span of the crossing, the magnitude of nonlinear effects are of primary concern. For steel design purposes, an approximate amplification factor is developed to take into account the geometric nonlinear effects.

Starting with the linearized beam-column differential equation and truncating power series of solution it can be shown (Chajes, 1974) that displacement magnification due to axial force second order effects can be approximated by the following expression:

$$v_2 = v_1 \frac{1}{1 - \frac{P}{Pcr}} \tag{10}$$

where v_2 e v_1 are respectively the vertical displacements of second and first order, P is the axial force and Pcr the critical force.

For the second order effect due to the prestressing force, the axial force is P_p = 143.7tf. In order to assess the critical force (Pcr_p) a linearized buckling analysis is performed. The pipeline is modeled as a beam simply supported in both

ends and at intermediate deviating stiffeners (Zielinski, 1992). The effective buckling length obtained is 12.86m, which is close to the largest unsupported length (13.05m), and the critical force is Pcr_p = 14961.9tf. Applying Eq. (10) the approximate amplification coefficient due to the prestress is c_p = 1.0097, which is very close to the finite element results for the case of water as distributed load 1.0098, see Tab. (3).

For the second order effect due to the water pressure, the effective axial force is the resultant of pressures on the pipe cross section, P_w = 56.73tf, while the effective buckling length is the tube length which is 38.6m (Feodosyev, 1997). The critical force is Pcr_w = 1662.7tf. By applying the relation given in Eq. (10) the approximate amplification coefficient due to water pressure is c_w = 1.0353. The total amplification (c_t) is given by:

$$c_t = c_p \cdot c_w \tag{11}$$

In the present case c_t = 1.045 which is a conservative approximation to the result from finite element analysis (1.034, see Tab. (3)).

7. Conclusions

An effective solution for elevated pipeline crossings up to 60m is externally prestressed steel tube. For the case study described herein it represents an economy of 12% with respect to the other alternatives.

Finite element models of localized stresses concentrations at intermediate stiffeners and stiffening ring supports are presented. For the loadings studied it can be concluded that the presence of flanges at the outer edge of stiffeners has no significant influence at the stresses. Due to the geometry deformation of the flanges it is not appropriate to model them as lumped bar elements attached to the edge of stiffener plates. A shell model with stiffeners is studied to avoid the damaging ovalization due to the prestressing force. In order to asses the stresses, a rational simplified method is developed. For the load levels considered the stresses are well below the yield limit of the structural steel used in the pipe. Second order effects are of primary concern therefore nonlinear analyses are studied. Caution should be exercised in modeling the water pressure. Water pressures must be applied as “follower” forces, otherwise a significant error is introduced rendering nonlinear displacement smaller than those of the linear analysis. Two sources of second order effects are identified: axial force due to prestressing and water internal pressure. A simplified rational method is presented to take into account both effects using critical loads as parameters. Computation of buckling force due to prestress may be based on the largest unsupported pipe length between stiffeners and deviators. Total pipe length should be used for buckling due to internal pressure, where the effective axial load is the resultant of pressures on the pipe cross section. The amplification factor obtained is very close to the results of full nonlinear finite element model and is therefore recommended for initial design purposes.

8. References

AWA, 1987, “AWA Manual M11”, American Water Works Association, Denver, USA.

Chajes, A., 1974, “Principles of Structural Stability”, Prentice Hall.

Cook, R. D., 1995, “Finite Element for Stress Analysis”, John Wiley & Sons.

Department of Public Works and Engineering, 1999, “City of Houston: Design Manual”.

Feodosyev, V. I., 1997, “Selected Problems and Questions in Strength of Materials”, Mir Publishers Moscow.

NB-599, 1987, “Forças devidas ao vento em edificações”, Associação Brasileira de Normas Técnicas.

MSC.Software Corporation, 2001, “MSC.Nastran Reference Manual”.

Pasternak, P., 1926, “Die praktische Berechnung biegefester Kugelschalen, Kreisrunder Fundamentplatten auf elastischer Bettung und Kreiszylindrischer Wandungen in gegenseitiger monolither Verbindung”, Zeitschrift fur angewandte Mathematik und Mechanik, Vol. 6, pp. 1.

Troitsky, M. S., 1982, “Tubular Steel Structures – Theory and Design”, The James F. Licoln Arc Welding Foundation.

Zielinski, Z. A. and Mobasher-Fard, H., 1992, “Strength and Behavior of Slender Steel Pipe Under Prestressing Force”, Journal of Structural Engineering, Vol. 118, No. 10.